Probing Conductivity in Polyelectrolyte/Nanoparticle Composite Films by Scanning Electrochemical Microscopy

Virginia Ruiz, Peter Liljeroth†, Bernadette M. Quinn and Kyösti Kontturi*

Laboratory of Physical Chemistry and Electrochemistry, Helsinki University of Technology, P.O. Box 6100, FIN-02015 HUT, Finland.

* Corresponding author. Email: bquinn@iki.fi

† Present address: Chemistry of Condensed Matter, Debye Institute, Utrecht University, PO Box 80000, 3508 TA Utrecht, The Netherlands.

ABSTRACT

An advanced electroanalytical technique, scanning electrochemical microscopy (SECM), is used as a new approach to measure both the lateral (in-plane) and cross-film electron transport in multilayer polymer/nanoparticle films. The sensitivity of SECM is such that the conductivity of a single nanoparticle monolayer can be quantified. The increase in SECM tip current with the number of polyelectrolyte/nanoparticle layer-pairs demonstrates that the subsequent layers are not electrically insulated from each other and that there is significant communication between nanoparticles in different layers.

Extensive recent interest has been directed towards the engineering of chemical assemblies of nanoscale dimensions for potential applications in nanotechnology.[1] Among the different techniques

developed to construct miniaturized devices, the layer-by-layer (LbL) self-assembly approach[2-5] has been the most widely employed, and has combined a number of nanoscopic materials[6-11] and polymers[6,11-14]. LbL polymer/nanoparticle assemblies are easily obtained by sequential electrostatic adsorption of layers of suitably functionalized nanoparticles on oppositely charged layers of polyelectrolytes. The resulting material is a nanoparticle-polymer hybrid, which combines the unique electronic[5,15] and optical[10,16] properties of nanoparticles with the mechanical properties of polymers. Developing methods to measure the electronic conductivities of such nanostructures is a crucial facet of this field. This paper reports on the use of an advanced electroanalytical technique, scanning electrochemical microscopy (SECM), as a new approach to measure both the lateral (in-plane) and cross-film electron transport in multilayer polymer/nanoparticle films (Figure 1). Previously, this technique has been used to probe lateral charge hopping in redox active monolayers,[17] the insulator-metal transition in an Ag nanoparticle monolayer[18] and local injection and lateral propagation of charge in ultra-thin polymer[19,20] and metal nanoparticle films[21]. One of the principal advantages of this technique compared with more conventional electroanalytical methods used to investigate the conductivity of nanoparticle assemblies[22-27] is that it is non-invasive, highly localized and does not require the film to be externally biased. Also, as the film is assembled on an inert substrate, the measured response is due solely to charge injection and lateral charge transport in the film. Here, it is further demonstrated that the technique is sufficiently sensitive to enable film conductance as a function of the number of consecutive layers assembled to be quantified.

Specifically, this paper describes the measurement of the lateral conductivity of composite ultra-thin films consisting of alternating layers of poly(allylamine hydrochloride) (PAH) and monolayer-protected gold clusters (MPC) with mixed monolayers of hexanethiolate and mercaptoundecanoic acid ligands (MUA-MPC) assembled on quartz slides. From the dependence of the amount of positive feedback on the number of polyelectrolyte/nanoparticle layer pairs, the extent of electronic communication between particles located in different polymer layers can be estimated.

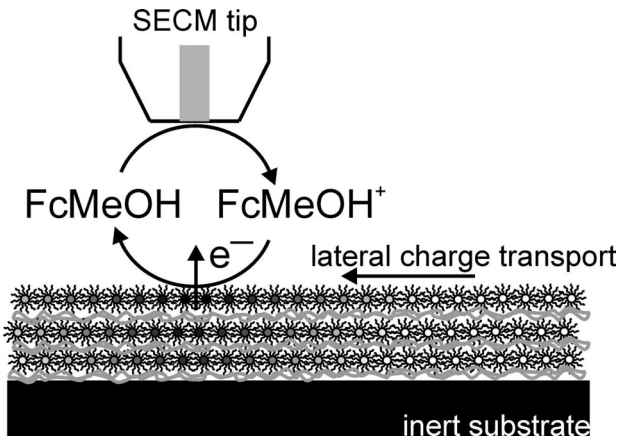


Figure 1. A schematic of the experimental setup used.

Hexanethiol stabilized gold particles were prepared as described previously.[11,28,29] The particles were sufficiently small and monodisperse to undergo quantized double layer charging at room temperature and core size (diameter 1.6 nm) was determined from the average spacing between successive charging peaks (ca. 250 mV as measured by cyclic voltammetry in 1,2-dichloroethane).[30] MPCs with mixed hexanethiolate/mercaptoundecanoic acid monolayers were prepared by place exchange reactions between hexanethiolate MPCs and mercaptoundecanoic acid.[11]

The protocol for the preparation of MPC/polymer multilayers[31] was as follows: prior to multilayer assembly, the quartz slides were cleaned thoroughly using a procedure described elsewhere.[3] The quartz slides were then silanized by immersion in a 5% solution of 3-aminopropyl-methyl-diethoxysilane in toluene for 15 h under an atmosphere of dry nitrogen followed by immersion (1 min) each in toluene, toluene/methanol (1:1), methanol and MQ water. For the adsorption of the first anionic layer, the substrates were immersed for 20 mins in an acidic solution of PSS (containing 2 mg ml^{-1}) at 0°C followed by rinsing with MQ water. Subsequent layers (PAH/MUA-MPCs) were assembled by alternately dipping the negatively terminated slide into the respective polymer (1 mg ml^{-1}) and MPC (1.5 mg ml^{-1}) solutions for 10 min.[11] The pH of the polycation solution was adjusted to 9.2 by the addition of 0.1 mol dm^{-3} NaOH solution. Growth of consecutive layers was followed by UV-vis spectrophotometry (HP 8452A diode array UV-vis spectrophotometer), showing that the films are built up in a linear manner (Supporting Information) with each layer containing approximately the same

amount of nanoparticles. The amount of nanoparticles in the film is given in equivalent monolayers, that is, the film absorbance divided by that of a monolayer.

The SECM experimental arrangement used is depicted in Figure 1. Measurements were performed using a commercially available SECM instrument (CHI-900, CH-Instruments, TX). A two-electrode arrangement was used, where a silver wire was used both as quasi-reference electrode and counter electrode. The working electrode used throughout was a 25 μm diameter Pt ultramicroelectrode (UME) and was prepared as previously described.[32] The ratio of the overall tip radius to that of the platinum disk, R_G, was 3.5, as determined from both optical micrographs and SECM approach curve experiments to insulating (PTFE) and conducting (Pt) substrates followed by fitting the results to the approximations provided by Amphlett and Denuault.[33]

A drop of aqueous solution containing varying concentrations of ferrocene methanol (FcMeOH) and 0.1 mol/dm^3 LiCl as the base electrolyte was pipetted onto the glass slide. Approach curves, where the current due to electrolysis of FcMeOH at the tip electrode is plotted as a function of distance d from the substrate, were then recorded as a function of both FcMeOH concentration and the number of layers assembled. At steady-state, the observed SECM response will be due to a combination of the diffusion flux in the solution and the flux due to lateral charge transport in the nanoparticle film. The diffusion flux is directly proportional to the concentration of the redox mediator in solution, c^b, and thus, in order to observe a measurable effect due to lateral transport, sufficiently low concentrations of the solution redox couple have to be used. Due to the large Coulomb gap of the MPCs used in this study, the nanoparticles in the film can be considered as multivalent redox species.[15,29,34] Furthermore, only the two redox states of the MPCs around the standard potential of solution redox couple will be involved. In addition, the transport mechanism between the particles is assumed to be thermally activated (non-coherent) tunnelling. If the film is thin compared to the radius of the SECM tip, it will not be polarized in the z-direction and a two-dimensional treatment is adequate. With these assumptions, the SECM feedback response can be modeled analogously to the previous lateral charge transport studies (Supporting Information).[17,35,36] The amount of positive feedback is determined by a dimensionless

parameter γD_r,[17,21,35,36] where $\gamma = \Gamma_{max}/(c^b a)$, $D_r = D_{surf} / D_{soln}$, Γ_{max} is the surface concentration of the nanoparticles in the top layer, a the radius of the microelectrode, D_{surf} diffusion coefficient characterizing electron transport in the film, and D_{soln} the diffusion coefficient of the solution redox couple. D_{surf} can be correlated to the conductivity of film as follows

$$\sigma = \frac{\Gamma_{max} F^2 D_{surf}}{RT\Delta z} = \frac{\gamma D_r F^2 a c^b D_{soln}}{RT\Delta z} \quad (1)$$

where R is the molar gas constant, T the temperature and Δz the thickness of the film.

The other relevant parameter that mainly affects the shape of the measured approach curve is the equilibrium constant K, of the electron transfer reaction between the solution redox couple and the nanoparticles in the film, which can be related to the difference between their standard potentials. The theory used to fit the approach curves has been described previously[21] and was extended here to include the effect of so-called back diffusion (diffusion from behind the plane of the microelectrode).[33]

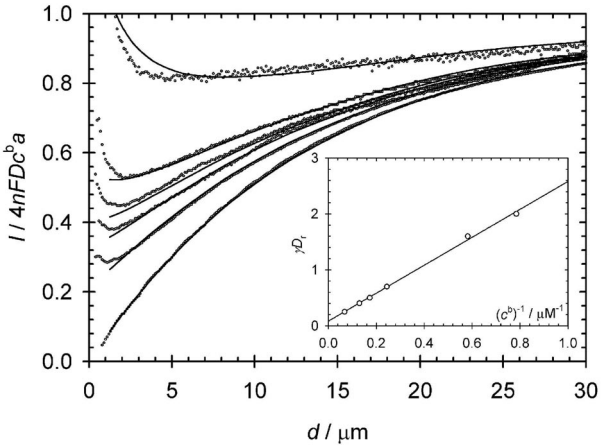


Figure 2. Examples of the measured approach curves (dots) along with the fits to the theory (solid lines) for 8 layers of polyelectrolyte/nanoparticle pairs. The concentration of the solution redox mediator, from top to bottom, 1.3 μmol dm^{-3}, 4.1 μmol dm^{-3} 7.7 μmol dm^{-3}, 14.7 μmol dm^{-3}, and 1.7 mmol dm^{-3}. The theoretical lines are generated with K = 0.3 and, from top to bottom, γD_r = 2, 0.7, 0.5, 0.4, 0.25, and 0. Inset shows γD_r as a function of the inverse of the concentration of the redox mediator in solution.

As an example, Figure 2 shows experimental approach curves and the corresponding fits to the theory recorded upon approaching a sample with 8 layers of PAH/MUA-MPC on quartz in solutions of different bulk concentrations of FcMeOH.[37] As the concentration of the redox mediator is lowered sufficiently, positive feedback is obtained due to charge transport inside the film. The inset in Figure 2 shows γD_r as a function of $(c^b)^{-1}$; the conductivity of the film can be calculated from the slope of the linear fit. All approach curves were fitted with K = 0.3. The sensitivity of SECM is such that the conductivity of a single monolayer can be quantified.[21] Examples of approach curves to a monolayer and the corresponding best fits to theory are given in Supporting Information. It should be stressed that approach curves were also recorded to a bare quartz substrate in the same concentration range of FcMeOH and positive feedback was never observed.

As expected, the level of positive feedback increases with increasing number of MPC-MUA layers and is easily visualized in approach curves given in Figure 3 obtained at the same concentration of redox mediator. From the values of γD_r obtained from fitting the experimental approach curves to the theory, it can be seen that doubling the number of layers results in less than a two-fold increase in γD_r.

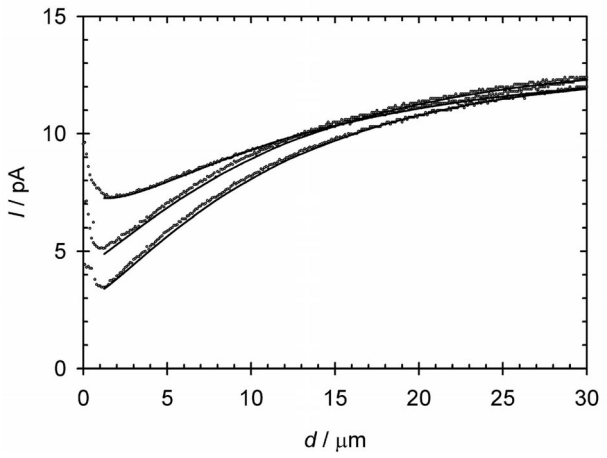


Figure 3. Approach curves at approximately identical concentrations of redox mediator to films composed of different numbers of polyelectrolyte/nanoparticle layers and the corresponding fits to theory; from top to bottom, 10 layers (c^b = 3.8 μmol dm^{-3}, γD_r = 0.6), 4 layers (c^b = 3.9 μmol dm^{-3}, γD_r = 0.3), and 2 layers (c^b = 3.8 μmol dm^{-3}, γD_r = 0.2).

In the case of a monolayer, from the slope of the plot of γD_r vs. $(c^b)^{-1}$, we can estimate the lateral conductivity $\sigma = 8.5\times10^{-5}\ \Omega^{-1}\text{cm}^{-1}$,[38] which is comparable to previous reports of similar systems.[23,25] For multilayer films, lateral and cross-plane electron transport contribute to the measured conductance. Due to film anisotropy, the rates of these two processes are not necessarily comparable. We therefore consider the slope of γD_r vs. $(c^b)^{-1}$ as an indication of the conductance of the nanoparticle/polyelectrolyte assemblies.

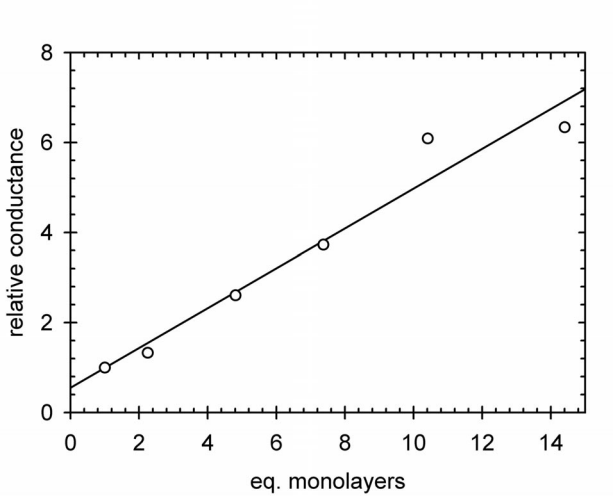


Figure 4. The relative conductance of the polyelectrolyte/nanoparticle assembly (conductance scaled by that of the first nanoparticle layer) as a function of the number of equivalent nanoparticle layers.

Figure 4 shows the measured conductance scaled by that of a monolayer as a function of the number of polymer/nanoparticle layers (given in terms of equivalent layers), with a linear increase of 44% per layer in the film thickness range considered. In a previous report, where the electron transport of comparable multilayers assembled on an electrode surface was probed, the absence of a ferrocene oxidation wave at the film-modified electrode was taken as an indication that the film was insulating.[11] The technique used relied on externally biasing a macroscopic electrode and probed cross-plane conductivity, i.e. how a solution redox species communicates with a metal electrode through a barrier film. With SECM, there is no net charge transfer through the film and consequently, counter-ion mobility into the film is not a limiting factor. Our results clearly show that the subsequent MPC layers are not electrically insulated from each other and that there is significant communication between MPCs

in different layers. If this were not the case, the measured conductance would be constant. Furthermore, if the resistance to charge transport in-plane and cross-plane were equal, the slope of the plot in Figure 4 should be unity. It can thus be concluded that while charge transfer between the nanoparticle planes does occur, it is hindered compared to the in-plane transport. However, a model for the structure of the polyelectrolyte/nanoparticle layer is needed in order to extract quantitative information of these two processes.

To summarize, we have demonstrated that SECM can be successfully used to probe both in-plane (lateral) and cross-plane electron transport in nanoparticle/polymer assemblies. It is perhaps the only technique that can allow ready discrimination between these competitive processes. This method is currently being applied to other nanoassemblies where the effect of the protecting ligand, the size of the metal core and the linker unit used on the resulting film conductance will be addressed.

Acknowledgement. This work is funded by the National Technology Agency, Finland, and the EU under the Sixth Framework Programme ("SUSANA", EU TMR network "Supramolecular Self-Assembly of Interfacial Nanostructures", contract number HPRN-CT-2002-00185).

Supporting Information Available. Plot of absorbance as a function of the dipping cycles, approach curves to a monolayer of assembled particles and additional information on the SECM experimental protocol and the theoretical framework. This material is available free of charge via the Internet at http://pubs.acs.org.

References

(1) *Nanoparticles and Nanostructured Films: Preparation, Characterization and Applications*; Fendler, J. H., Ed.; Wiley-VCH: Weinheim, 1998, pp 468.

(2) Iler, R. K. *J. Colloid Interface Sci.* **1966**, *21*, 569.

(3) Decher, G.; Hong, J. D. *Thin Solid Films* **1992**, *210*, 831.

(4) Decher, G. *Science* **1997**, *277*, 1232.

(5) Fendler, J. H. *Chem. Mater.* **2001**, *13*, 3196.

(6) Liu, Y.; Wang, Y.; Claus, R. O. *Chem. Phys. Lett.* **1998**, *298*, 315.

(7) Donath, E.; Sukhorukov, G. B.; Caruso, F.; Davis, S. A.; Möhwald, H. *Angew. Chem. Int. Ed.* **1998**, *37*, 2202.

(8) Mamedov, A. A.; Kotov, N. A. *Langmuir* **2000**, *16*, 5530.

(9) Mamedov, A.; Ostrander, J.; Aliev, F.; Kotov, N. A. *Langmuir* **2000**, *16*, 3941.

(10) Mamedov, A. A.; Belov, A.; Giersig, M.; Mamedova, N. N.; Kotov, N. A. *J. Am. Chem. Soc.* **2001**, *123*, 7738.

(11) Hicks, J. F.; Young, S.-S.; Murray, R. W. *Langmuir* **2002**, *18*, 2288.

(12) Lvov, Y.; Munge, B.; Giraldo, O.; Ichinose, I.; Suib, S. L.; Rusling, J. F. *Langmuir* **2000**, *16*, 8850.

(13) Musick, M. D.; Keating, C. D.; Keefe, M. H.; Natan, M. J. *Chem. Mater.* **1997**, *9*, 1499.

(14) Wang, T. C.; Rubner, M. F.; Cohen, R. E. *Langmuir* **2002**, *18*, 3370.

(15) Templeton, A. C.; Wuelfing, W. P.; Murray, R. W. *Acc. Chem. Res.* **2000**, *33*, 27.

(16) Antipov, A. A.; Sukhorukov, G. B.; Donath, E.; Möhwald, H. *J. Phys. Chem. B* **2001**, *105*, 2281.

(17) Zhang, J.; Slevin, C. J.; Morton, C.; Scott, P.; Walton, D. J.; Unwin, P. R. *J. Phys. Chem. B* **2001**, *105*, 11120.

(18) Quinn, B. M.; Prieto, I.; Haram, S. K.; Bard, A. J. *J. Phys. Chem. B* **2001**, *105*, 7474.

(19) Mandler, D.; Unwin, P. R. *J. Phys. Chem. B* **2003**, *107*, 407.

(20) Zhang, J.; Barker, A. L.; Mandler, D.; Unwin, P. R. *J. Am. Chem. Soc.* **2003**, *125*, 9312.

(21) Liljeroth, P.; Quinn, B. M.; Ruiz, V.; Kontturi, K. *Chem. Commun.* **2003**, 1570.

(22) Chen, S. *J. Phys. Chem. B* **2000**, *104*, 663.

(23) Wuelfing, W. P.; Green, S. J.; Pietron, J. J.; Cliffel, D. E.; Murray, R. W. *J. Am. Chem. Soc.* **2000**, *122*, 11465.

(24) Wuelfing, W. P.; Murray, R. W. *J. Phys. Chem. B* **2002**, *106*, 3139.

(25) Zamborini, F. P.; Leopold, M. C.; Hicks, J. F.; Kulesza, P. J.; Malik, M. A.; Murray, R. W. *J. Am. Chem. Soc.* **2002**, *124*, 8958.

(26) Hicks, J. F.; Zamborini, F. P.; Osisek, A. J.; Murray, R. W. *J. Am. Chem. Soc.* **2001**, *123*, 7048.

(27) Hicks, J. F.; Zamborini, F. P.; Murray, R. W. *J. Phys. Chem. B* **2002**, *106*, 7751.

(28) Brust, M.; Walker, M.; Bethell, D.; Schiffrin, D. J.; Whyman, R. *Chem. Commun.* **1994**, 801.

(29) Quinn, B., M.; Liljeroth, P.; Ruiz, V.; Laaksonen, T.; Kontturi, K. *J. Am. Chem. Soc.* **2003**, *125*, 6644.

(30) Hicks, J. F.; Templeton, A. C.; Chen, S.; Sheran, K. M.; Jasti, R.; Murray, R. W.; Debord, J.; Schaaff, T. G.; Whetten, R. L. *Anal. Chem.* **1999**, *71*, 3703.

(31) 3-aminopropyl-methyl-diethoxysilane (Fluka), poly(sodium 4-styrenesulfonate) (M_w ~ 1800 g mol^{-1}, PolySciences, Inc.) and poly(allylamine hydrochloride) (M_w ~ 70000 g mol^{-1}, Aldrich) were used as received. All other chemicals used were of the highest commercially available purity. Aqueous solutions were prepared using MQ®-treated water (Millipore, US).

(32) Bard, A. J.; Fan, F. R. F.; Mirkin, M. V. Scanning electrochemical microscopy. In *Electroanalytical Chemistry*; Bard, A. J., Ed.; Marcel Dekker: New York, 1994; Vol. 18; pp 243.

(33) Amphlett, J. L.; Denuault, G. *J. Phys. Chem. B* **1998**, *102*, 9946.

(34) Chen, S.; Murray, R. W.; Feldberg, S., W. *J. Phys. Chem. B* **1998**, *102*, 9898.

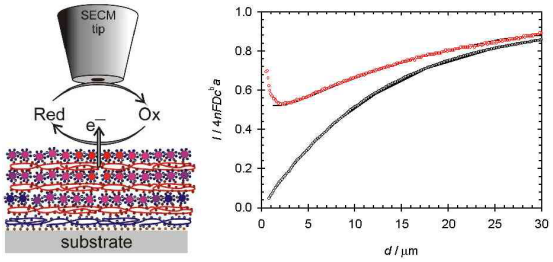
(35) Unwin, P. R.; Bard, A. J. *J. Phys. Chem.* **1992**, *96*, 5035.

(36) Slevin, C. J.; Unwin, P. R. *J. Am. Chem. Soc.* **2000**, *122*, 2597.

(37) The SECM approach curves were carried out at an approach speed of 1 μm s^{-1}. Approach curves were always also recorded both in the absence of the redox couple and to a bare glass substrate in the concentration range of the redox mediator use. Detailed information can be found in the Supporting Information.

(38) D_{soln} = 7×10^{-6} cm^2 s^{-1}; a = 12.5×10^{-4} cm; Δz = 1.6 nm was taken as the diameter of the nanoparticles.

Table of Contents Graphic:


SECM
tip
Red
e–
Ox
substrate
1.0
0.8
0.6
0.4
0.2
0.0
0
5
10
15
20
25
30
d / μm